International Journal of Applied Engineering Research ISSN 0973-4562 Volume 12, Number 19 (2017) pp. 8844-8853

Classification of Textures Using a New Descriptor Circular and Elliptical-LBP (CE-ELBP)

K. Subba Reddy
Research Scholar, Jawaharlal Nehru Technological University, Anantapur, Ananthapuramu, Andhra Pradesh, India.
Associate Professor, Deparof CSE , RGMCET, Nandyal, Andhra Pradesh, India.

V. Vijaya Kumar
Dean, Department of Computer Science and Engineering & Informations Technology, Director-CACR, Anurag Group of Institutions (Autonomous), Hyderabad, India.

A.P. Siva Kumar
Professor, Department Computer Science and Engineering, Jawaharlal Nehru Technological University, Ananthapuramu, Andhra Pradesh, India.

Abstract

The Local binary Pattern (LBP) is a very simple and popular approach, and it played a vital role in many image processing applications. LBP captures isotropic structural information. The LBP completely fails in representing anisotropic information. Later, to represent anisotropic, horizontal elliptical LBP (H-ELBP) and vertical elliptical LBP (V-ELBP) are derived, however they derived only partial anisotropic information. To derive complete anisotropic information these two ELBPs are concatenated and it increases the feature vector size by two folds when compared to LBP. To capture both isotropic and anisotropic structural information, one needs to concatenate the histograms of LBP, H-ELBP and V-ELBP and this process increases the feature vector size into three folds when compared with LBP. We present a novel Feature Extraction method known as "circular and elliptical-LBP (CE-ELBP)" and a new variant of local binary pattern (LBP) and elliptical LBP (ELBP). The CE-LBP captures both isotropic and anisotropic structural information with a feature vector size equivalent to LBP. The CE-LBP quantizes/places the multi-structure information of LBP and ELBP (H-ELBP and V-ELBP) and derives a unique CE-LBP code that represents the complete set of micro patterns. The distinct advantages of CE-LBP are its ease in implementation, invariance to monotonic illumination changes and low computational complexity. The CE-LBP is tested on well-known databases i.e., Brodtaz, UIUC and Outex using machine learning classifiers. The classification results are compared with conventional LBP, H-ELBP, V-ELBP and combination of these descriptors. The uniform patterns are also derived on CE-LBP and classification results are derived and compared. The results indicate the efficacy of the proposed method.

Keywords: Isotropic; Anisotropic; horizontal elliptical LBP; vertical elliptical LBP;

INTRODUCTION

Local Binary Patterns (LBP) have emerged as one of the most prominent and widely studied local texture descriptors in the field of computer vision and pattern recognition. This is mainly because of the merits of LBP i.e., simplicity, ability to capture image micro-structures, and robustness to illumination variations. A vast number of LBP variants were proposed for a diverse range of applications e.g., texture classification [1, 2, 3, 4], image retrieval [5, 6, 7], dynamic texture recognition [8, 9, 10], face image analysis [11] scene recognition [12 -15], object detection [16, 17], human detection [18, 19], biomedical image analysis [20, 21], and many others [22-28].

As per our knowledge, only few authors carried out literature survey on LBP [5, 29, 30, 31, 32]. The literature surveys on LBP [29, 30], miss recent variants and do not include experimental investigations and where as the other papers [5, 6, 30, 31, 32] reviewed LBP variants and carried out experimental evaluation. In [5, 6, 7] the survey on LBP was carried out mainly based on its role in texture retrieval. The surveys on LBP [31, 32] were carried out on texture image classification. Recently, a more systematic survey on LBP with more number of variants and investigation on more number of data sets were carried out [33].A number of image descriptors were proposed by combining LBP with other descriptors. Gabor filters are used as preprocessing tools before LBP computation and these two provide complementary information: LBP captures small and fine details, while Gabor filters encode appearance information over a broader range of scales. The prominent work on this is, Local Gabor Binary Pattern (LGBP) [34].The CLBP descriptor [35] is derived by combining multiple LBP features i.e. CLBP_S, CLBP_M and CLBP_C. Based on the local differences in LBP two complementary components i.e., the Sign (CLBP_S) and Magnitude (CLBP_M) are derived. By using global threshold

and by considering the importance of grey level value of centre pixel in providing the discriminative information, the CLBP-C is derived. Later The CMLBP [36] approach are derived based on CLBP.

The advantage of LBP is, it can easily combine with other features to derive significant local texture information. To achieve rotation invariance globally, the LBP Histogram Fourier features (LBPHF) are derived by combining LBP with Discrete Fourier transform (DFT) [37]. LBPHF is combined with the CLBP_S and CLBP_M descriptors [35] to improve its distinctiveness further. Inspired by promising results of LBP and its variants, several researchers have developed local descriptors including LPQ [38], WLD [39], HGPP [40], LHS [41] and LFD [42, 43].

In the literature, different topologies were introduced on LBP,to capture different structural information. The Local Line Binary Pattern (LLBP) [44], which uses lines in vertical and horizontal directions for LBP computations. Other geometries, such as line and disk, were explored in local quantized pattern (LQP) [45]. The LQP allows larger local neighborhoods, and by this, it provides an increase in discriminative power with an increase in number of quantization levels and dimension. The "Elliptical local binary patterns (ELBP) [46], also generalized in [47] to parabolic, hyperbolic, and spiral neighborhood topologies, ELBP was proposed by Shu Liao et.al. [46]. The ELBP, exploits elliptical patterns whereas the LBP derives circular patterns of the image.

The circular neighborhood of LBP, allows deriving rotation invariant features, however it misses to represent anisotropic structural information, which may be an important feature for many applications. To exploit anisotropic structure information, ELBP's are derived. However, they completely fail in representing circular structures. This paper proposes, a new way to incorporate both isotropic and anisotropic information into LBP structure. For this, we extract design rule from handcrafted LBP and ELBP structures, i.e., computing the average gray values of two neighboring pixels as a single value.

The present paper is organized as follows. The section two describes the proposed method and section three presents' results and discussions and the conclusions are presented in section 4.

DERIVATION OF ISOTROPIC AND ANISOTROPIC STRUCTURE INFORMATION USING A NEW VARIANT: CIRCULAR AND ELLIPTICAL-LBP (CE-LBP)

The basic LBP structure consists of a circular neighborhood(derived on a 3 x 3 neighborhood) with eight nearest neighbors [47] or d neighbors in a circle of radius 'R=1"[46]. The advantage of circular neighborhood is that it achieves rotational invariance and preserves isotropic information [46].The basic LBP was later extended with more number of sampling points (d), with different radius(R), different topologies and dimensions of the neighborhood but retaining the circular shape only. The isotropic structure of LBP may not be suitable for all applications. The anisotropic structural information is also an important feature for many image processing applications especially in face recognition, age classification etc., where the human eyes and mouth are basically anisotropic structures. To acquire this important feature, many researchers used elliptical local binary patterns (ELBP). LBP itself, is a special case of ELBP. The present paper derives a completely new variant of LBP and ELBP, called CE-LBP, to capture both isotropic and anisotropic structural information. The block diagram of CE-LBP is illustrated in Figure 2.The micro information of the texture in ELBP model is usually captured by using horizontal and vertical ELBP's.

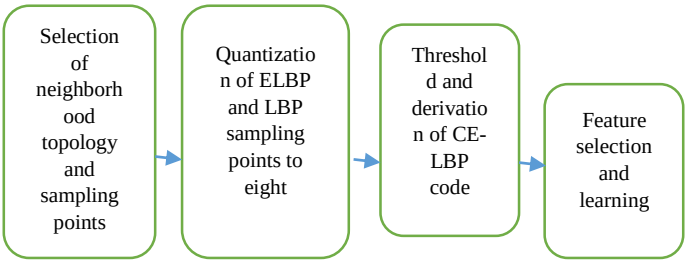

Figure 1: The extraction process of CE-LBP.

The conventional LBP[4] represents the spatial structure of the local texture. The local patterns are derived in LBP, by thresholding the 8-neighboring pixels of 3x3 neighborhood with the value of centre pixel(Figure 2).

d_1	d_2	d_3
d_8	d_c	d_4
d_7	d_6	d_5

Figure 2: 3x3 neighborhood.

The LBP considers only sign information, to derive local binary patterns of the neighborhood, because of which the LBP is invariant to monotonic illumination changes. The LBP code of a pixel (x_c,y_c) is defined as :

$$LBP_{d,R}(x_c, y_c) = \sum_{i=1}^{n} S(d_i - d_c) * 2^{i-1}$$

$$\text{where } S(x) = \begin{cases} 1, & x \geq 0 \\ 0, & x < 0 \end{cases} \quad (1)$$

Where d_c is the intensity value of centre pixel (x_c,y_c), d_i corresponds to the intensities of d-neighboring pixels located on a circle of radius R centered at d_c. In practice, the neighboring pixels are sampled on a circle. The neighboring pixels which do not fall exactly on the circle, are estimated by interpolation. The $LBP_{d,R}(xc,yc)$ derives an unique decimal number ranges from 0 to 2^d-1. Figure 3 represents various

multi-resolution circular symmetric neighbors' sets of LBP with different values of d and R.

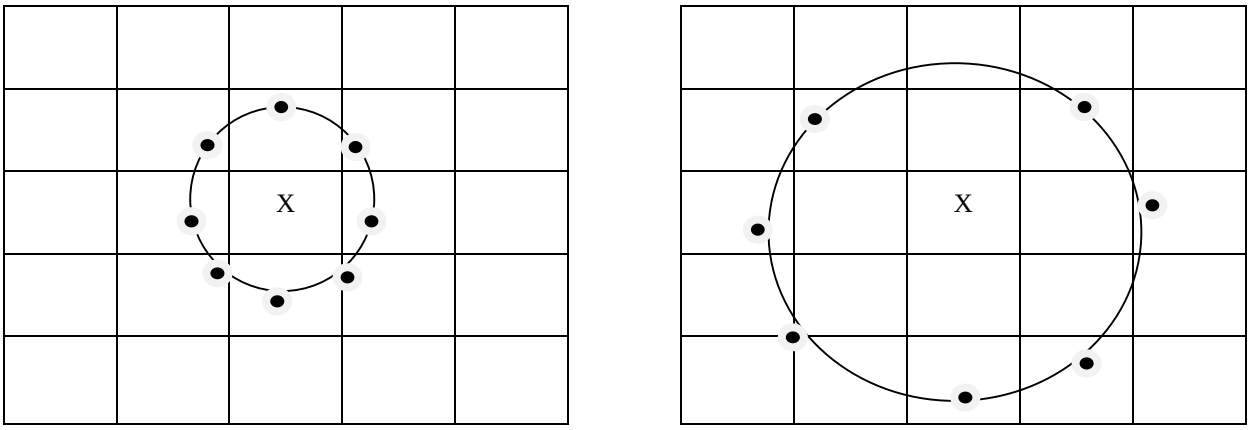

(a) (8,1) (b) (8,2)

Figure 3: LBP with different resolutions (a) 3x3 neighborhood (8,1) (b) 5x5 neighborhood (8,2).

In ELBP, the distribution of sampling pixels form an elliptic shape. To represent LBP, we need to have two parameters i.e., the radius R of the neighborhood and the number of sampling pixels 'd'. Three parameters i.e., horizontal (x-axis) radius of ellipse denoted as 'hR', the vertical (y-axis) radius of ellipse denoted as 'vR' and the number of sampling points 'd' of the elliptical neighborhood are required to represent ELBP. Based on the relationship between hR and vR two ELBPS i.e., horizontal ELBP (H-ELBP) (Figure 4.b) and vertical ELBP (V-ELBP) (Figure 4.c) are derived to represent the complete anisotropic information. In ELBP, the neighboring pixel co-ordinate (x_i, y_i) of the centre pixel (x_c,y_c) is derived, based on the following equations that represent ellipse.

$$angle - step = 2 * \pi/n \quad (2)$$

$$x_i = x_c + hR * (\cos(i-1) * angle - step) \quad (3)$$

$$y_i = x_c + vR * (\cos(i-1) * angle - step) \quad (4)$$

If hR = vR, then ELBP becomes LBP, hR>vR, then ELBP represents H-ELBP otherwise when hR<vR the ELBP becomes V-ELBP. The ELBP is denoted as $ELBP^{d,hR,vR}$.

The unique decimal code for $H - ELBP^{d,HR,VR}(x_c, y_c)$ and V-$ELBP^{d,hR,vR}$ (x_c,Y_c) at each centre pixel (x_c,y_c) is derived based on equation 5 and 6.

$$ELBP^{d,hR,vR}(x_c, y_c) = \sum_{i=1}^{P} s\left(d_i^{n,hR,vR} - d_c\right).2^{i-1} \quad (5)$$

WhereS(x) is defined as

$$S(x) = f(x) = \begin{cases} 1, & if x \geq 0 \\ 0, & x < 0 \end{cases} \quad (6)$$

The decimal codes of conventional $LBP_{1,2}$,H-$ELBP^{8,2,1}$ and V-$ELBP^{8,2,1}$ ranges from 0 to 2^{d-1} (255). To capture the complete anisotropic structure information, we should concatenate the histograms ofH-$ELBP^{8,2,1}$ and V-$ELBP^{8,2,1}$codes. The dimension of these histograms ranges from 0 to 511, however, it completely misses the isotropic information. The $LBP_{8,1}$captures the complete isotropic information with a histogram bin range of 0 to 255. Therefore, to capture both isotropic and anisotropic information of the textures, one should integrate/ concatenate both H-ELBP, V-ELBP with LBP. In this case, the number of bins of histogram ranges from 0 to 767 which increases the dimensionality to a huge extent. To overcome this dimensionality problem and to capture both isotropic and anisotropic structural information, the present paper derived elliptical and circular LBP(EC-LBP) or isotropic and anisotropic structural LBP (IA-LBP).

The following Figure 4 give the circular neighborhood and elliptical neighborhood (both horizontal and vertical) pixel windows.

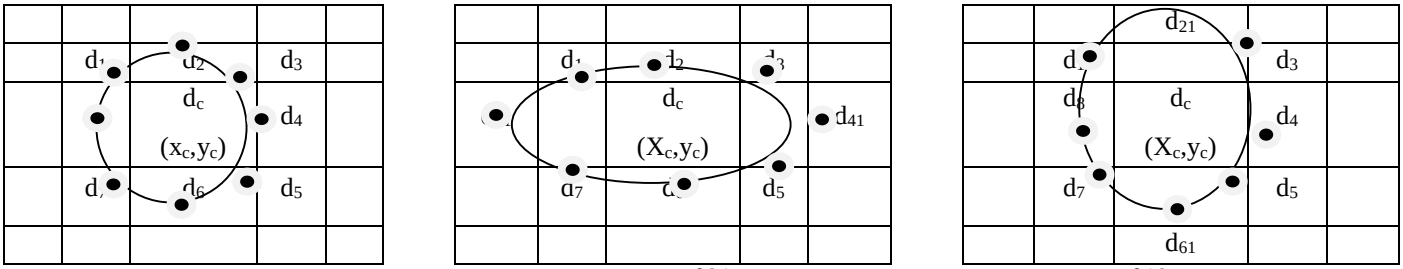

(a): $LBP_{1,2}$ (b): H-ELBP ^{8,2,1} (c): V-ELBP ^{8,1,2}

Figure 4: The representation of basic LBP, H-ELBP and V-ELBP.

The12-neighborhood pixels (d_1, d2, …, d_8, d_{41}, d_{81}, d_{21}, d_{61}) around centre pixel $d_c$are required to form the basic LBP, H-ELBP and V-ELBP (Figure 4).Out of these, the diagonal pixels of LBP d_1, d_3, d_5 andd_7 are common among the three local patterns i.e. the LBP, H-ELBP and V-ELBP. The neighborhood pixels $d_2$andd_6 are common among LBP and H-ELBP (Figure 4.b). The neighborhood sample points d_4 andd_8 are common among V-ELBP and LBP (Figure 4.a).

To capture both isotropic and anisotropic structural information, we need to consider all 12 sampling points around d_c, and in this case, the dimension of this structure ranges from 0 to 2^{12}-1 i.e. 0 to 4095 (Figure 5 (a)). However if one concatenates the histogram bins of LBP with H-ELBP and V-ELBP, the range of histogram bins will be from 0 to 767.

		d_{21}		
	d_1	d_2	d_3	
d_{81}	d_8	d_c	d_4	d_{41}
	d_7	d_6	d_5	
		d_{61}		

(a): The sampling points of LBP and ELBP

d_1	$(d_2+ d_{21})/2$	d_3
$(d_8+ d_{81})/2$	d_c	$(d_4+ d_{41})/2$
d_7	$(d_6 +d_{61})/2$	d_5

(b): The quantized sampling points of CE-LBP

Figure 5: The quantization process of sampling points of CE-LBP over the centre pixel d_c.

The aim of this paper is to derive circular and elliptical LBP(CE-LBP) that captures the total isotropic and anisotropic structure information with a minimum feature size. For this, the proposed CE-LBP quantizes, the total number of neighboring points around (x_c, y_c), that are required for LBP, H-ELBP and V-ELBP, into 8- neighboring points and derives a unique code for CE-LBP as shown in Figure 5 (b).

For this the CE-LBP combines the two top pixels (d_2 andd_{21}), two bottom pixels (d_6 andd_{61}), two left pixels (d_8 andd_{81}) and two right pixels (d_4 andd_{41}) of d_c into one and represents the CE-LBP in a 3 x 3 a neighborhood(Figure 5 (b)) using the following equations

$$d_2 = int((d_2 + d_{21})/_2) \quad (6)$$

$$d_4 = int((d_4 + d_{41})/_2) \quad (7)$$

$$d_6 = int((d_6 + d_{61})/_2) \quad (8)$$

$$d_8 = int((d_8 + d_{81})/_2) \quad (9)$$

Using the above the present paper derived a CE-LBP code of a pixel d_c with co-ordinate position (x_c, y_c) as

$$\mathrm{CE-LBP}_{(d,R1,R2)} = \sum_{i=1}^{8} S(d_i - d_c) * \ 2^{i-1} \quad (10)$$

with

$$s(x) = \begin{cases} 1, \ if\ x \geq 0 \\ 0, \ \text{if}\ x < 0 \end{cases} \quad (11)$$

where d_c and d_i represent the intensity values of the centre and neighboring pixels; The R_1 corresponds to the 'R' of LBP, the 'vR' of H-ELBP and 'hR'- of V-ELBP; The R_2 corresponds to 'hR' of H-ELBP and 'vR'- of V-ELBP. The range of CE-$LBP_{(8,1,2)}$is from 0 to 255, with complete isotropic and

anisotropic information. The working mechanism of CE-LBP $_{(8,1,2)}$ is illustrated in Figure 6. We move the 5x5 block from left-to-right and top-to-bottom throughout the image to compute CE-LBP$_{(8,1,2)}$ code with 1 pixel as the step-length. In Figure 6 the centre pixel is replaced with CE-LBP$_{(8,1,2)}$ code 119.

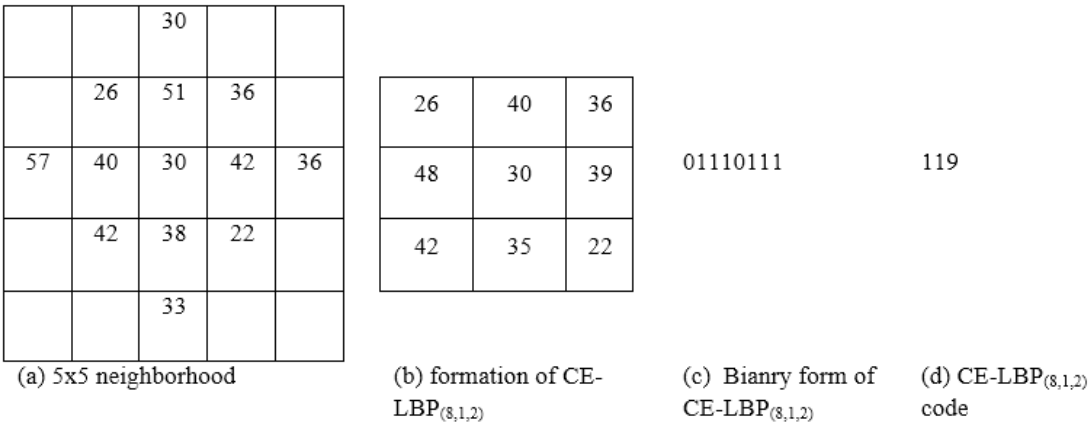

Figure 6: Derivation of CE-LBP $_{(8,1,2)}$ from a 5x5x neighborhood.

In the literature after studying the conventional LBP trends on number of texture and facial images, it is observed that certain type of LBP represents more 90% of the windows. They are termed as uniform LBP(ULBP) and they are considered as fundamental units of textures. A pattern is uniform if the circular sequence of bits contains no more than two transitions from one to zero, or zero to one. There are 58 ULBPs on a neighborhood with d=8 and R=1. The number of ULBP's over a neighborhood with d number of sampling points is given by d x (d-1) +2. The ULBP approaches considered the remaining 198 LBP as non-ULBP (NULBP) and considered them miscellaneous and assigned them an unique code. The ULBP approach reduced the LBP codes from 0 to 255 to 0 to 58 and the code zero is assigned to all 198 NULBP's. In the similar way, the present paper evaluated the uniform codes on CE-LBP(CE-ULBP) and evaluated texture classification.

RESULTS AND DISCUSSIONS

To investigate the classification accuracy, we have identified three well known and popular texture databases i.e. Brodtaz[48], UIUC[49] and Outex[50].The images of these databases are captured under varying conditions like lighting, illumination and varying sizes. Each database consists of various classes and each class consists of various images. This paper compared the proposed novel descriptors with LBP, H-ELBP, V-ELBP and concatenation of H-ELBP and, V-ELBP (HV-ELBP). Further, this paper also evaluated Uniform LBP (ULBP) on the above descriptors and compared the classification rates of the proposed novel CE-ULBP with ULBP, H-EULBP, V-EULBP andHV-EULBP on the above natural databases. This paper used the machine learning classifiers Ibk, multilayer perceptron, and Liblinear for classification purpose.

This paper selected30 different homogeneous texture images from Brodtaz database with a dimension of 640 x 640 pixels. The sample images are shown in Figure 7. This paper divided each image into 25 non-overlapped texture images of size 128x128. This results a dataset of 750 images (30 x 25). The proposed classifiers were trained by using 10 samples of each class (30 x 10=300 images in total) and the remaining 15 samples per class were used for validation (30 x 15=450 images in total).

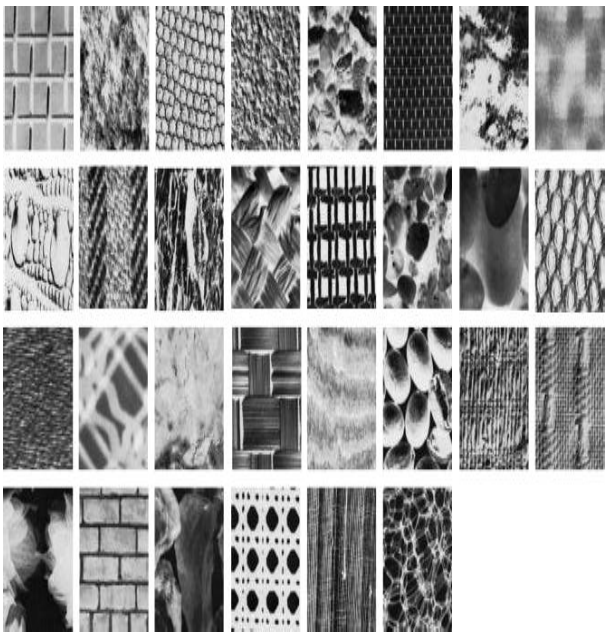

Figure 7: Samples of the 30 classes randomly selected from the Brodatz database.

The Outex database contains two test suits: Outex-TC-10(TC12-000) and Outex-TC-12(TC12-001). Two subsets of the Outex dataset, test suite TC10 (also known as Outex_TC_00010 in [39]) and test suite TC12 (also known as Outex_TC_00012 in [39]) are used for texture classification. Both TC10 and TC12 are composed of 24 texture classes of images under 128 × 128 resolutions for nine rotation angles (0°, 5°, 10°, 15°, 30°, 45°, 60°, 75°,and 90°) and on each rotation angle, there are 20 images. These images are captured under three illumination conditions namely 1. "inca' 2. t184 3. Horizon. The total number of images in TC10 and TC12 are 4320 and 9120, respectively. All images in TC10 are under the same illuminant inca, and this leads to 4320 (24 × 9 × 20 = 4320) images in total. , There are 480 images in TC12 under inca in a single direction (24 x 20=480). There are 4320 t184 images and 4320 horizon images in TC12 under nine rotation angles (24 x 20 x 9=4320). This leads to a total of 9120 images in TC12. Both TC10 and TC12 share the same training dataset of the 480 "inca" images but use different test datasets.

For the TC10 dataset, with illumination condition "inca" with 0^o of rotation (24 x 20=480 image), is used for training purpose in the present paper. The reaming images with other 8-rotations are used for testing (24 x 8 x 20=3840 images). For TC-12 dataset, the 24 x 20 images of illumination "inca" and rotation angle zero degrees are adopted for the training process. All the 24 x 20 x9 samples captured under illumination (tl84 or horizon) are used as test data for TC12 dataset. The sample images from Outex database are shown in Figure 8.

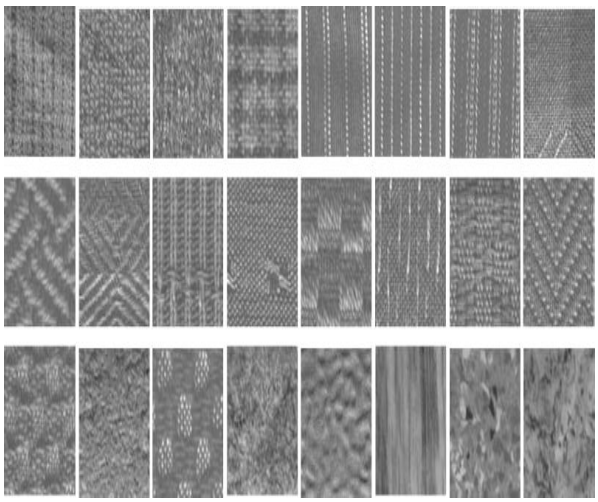

Figure 8: The sample images of 24 classes from Outex database.

The sample images of UIUC database are shown in Figure 9. This database includes 25 classes and each class consists of 40 images. This resultsa total of 1000(25x40) texture images. The size of each image is 640x480. In our experiments we have partitioned 640 x 480 images into 15 non-overlapped images of size 128x128. This leads to a total of 15000 (25x 40 x 15) images and a total of 600 (40 x 15=600) images per class. In our texture classification experiments, 300 training images are randomly chosen from each class, while the remaining 300 images are used as test set.

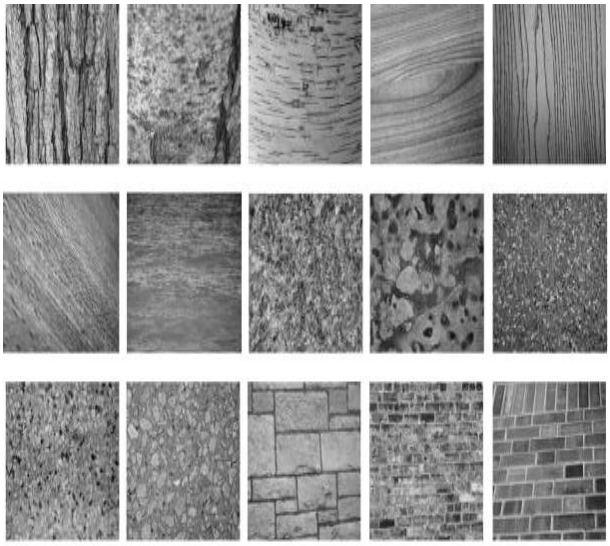

Figure 9: Samples of the 25 classes from the UIUC database.

The texture classification results of the two proposed methods i.e. CE-LBP and CE-ULBP are compared with LBP and ELBP methods and listed in Table 1,2 and 3 for Brodtaz[48], UIUC[49] and Outex[50] databases respectively. The following are noted down.

From Table 1 i.e. the classification results on the Brodtaz textures, the following findings are noted down. The proposed CE-LBP outperformed the LBP, H-ELBP, V-ELBP and concatenation of horizontal and vertical ELBP models. The basic reason for this, the CE-LBP captures the both isotropic and anisotropic structure information.

1. The isotropic structural model i.e. the LBP attained an average of 3% high classification rate than the partial anisotropic models: H-ELBP or V-ELBP.
2. The complete anisotropic structural information is obtained in the present paper by concatenating the H-ELBP and V-ELBP and this descriptor attained almost similar classification rate of LBP with an increase of dimensionality by two folds.
3. The proposed CE-LBP attained high classification rate of above 3%, 5% and 4% over LBP, partial anisotropic structures (H-ELBP and V-ELBP) and complete anisotropic structure HV-ELBP respectively.
4. The above trend is repeated on ULBP's. The ULBP and concatenation of Horizontal and Vertical EULBP(HV-EULBP) attained almost same classification rate, however the feature vector size is doubled in the case of HV-EULBP descriptor.
5. The proposed CE-ULBP descriptors achieved an average of 6% high classification rate than conventional ULBP and also on other ELBP's.

6. The proposed CE-LBP and CE-ULBP have exhibited high classification rate on all three classifiers when compared to other conventional descriptors.

The experimental results on various variants of LBP on UIUC dataset using various classifiers are placed in Table 2 and the following are noted down.

1. The proposed CE-LBP attained a better classification rate on all three classifiers when compared to LBP and ELBP descriptors.
2. The isotropic structural descriptor attained an average 3% of high classification rate when compared to partial anisotropic structures; however the complete anisotropic structural descriptor (HV-ELBP) attained almost the same classification rate of LBP.
3. In case of uniform patterns, the CE-ULBP showed a 3% low classification rate when compared to CE-LBP. The CE-LBP has displayed an average of5 % high classification rate when compared to H-ELBP and V-ELBP and an average of10% high classification rate when compared to ULBP and HV-EULBP.

The Table 3 displays the experimental results on the Outex dataset and from this the following are noted.

1. The partial anisotropic models: H-ELBP or V-ELBP exhibited a low performance of 1% when compared to LBP.
2. The HV-ELBP has shown slightly high classification rate than LBP model.
3. The proposed CE-LBP attained high classification rate of more than5% and 6%, over LBP or HV-LBP and partial anisotropic structures (H-ELBP or V-ELBP) respectively.
4. The HV-EULBP attained slightly better classification rate than ULBP. And both these descriptors achieved a 2% higher classification rate when compared to H-EULBP or V-EULBP descriptors.
5. The proposed CE-ULBP descriptors achieved an average of 8% high classification rate than conventional ULBP and also on other ELBPs.

Table 1: Classification rate on Brodtaz dataset.

S.No	Name of the method	Liblinear	Multilayer Perceptron	Average
1	LBP	90.02	91.82	90.92
2	H-ELBP	89.48	90.01	89.75
3	V-ELBP	88.28	89.24	88.76
4	H U V-ELBP	90.24	90.84	90.54
5	CE-LBP	93.72	94.68	94.20
6	ULBP	86.20	87.25	86.73
7	H-ULBP	85.44	84.23	84.84
8	V-ULBP	86.32	85.27	85.80
9	HUV –ULBP	87.21	87.28	87.25
10	CE-ULBP	92.48	93.25	92.87

Table 2: Classification rate on UIUC dataset.

S.No	Name of the method	Liblinear	Multilayer Perceptron(MLP)	Average
1	LBP	54.65	56.27	55.46
2	H-ELBP	52.25	53.89	53.07
3	V-ELBP	53.08	54.25	53.67
4	HV-ELBP	54.08	55.96	55.02
5	CE-LBP	60.72	62.88	61.80
6	ULBP	52.28	53.18	52.73
7	H-ULBP	49.97	52.16	51.07
8	V-ULBP	48.67	50.12	49.40
9	HUV –ULBP	53.67	55.27	54.47
10	CE-ULBP	57.21	60.02	58.62

Table 3: Classification rate on Outex dataset.

		TC-10		TC-12 ’t’		TC-12 ‘h’	
S.No	Name of the method	LL	MLP	LL	MLP	LL	MLP
1	LBP	84.87	85.52	65.19	66.32	64.03	65.63
2	H-ELBP	83.45	84.68	64.18	65.36	63.23	64.58
3	V-ELBP	84.02	85.67	63.76	64.85	63.06	64.85
4	HV-ELBP	85.05	86.36	64.28	65.98	64.48	65.39
5	CE-LBP	90.24	91.28	73.89	74.68	72.91	73.68
6	ULBP	79.98	81.21	61.90	62.38	60.01	61.35
7	H-ULBP	80.24	81.86	59.82	60.35	58.84	59.68
8	V-ULBP	81.03	82.34	58.74	59.68	58.91	59.48
9	HUV –ULBP	81.76	82.65	60.91	61.48	60.25	61.35
10	CE-ULBP	87.84	88.91	70.94	71.63	70.21	72.15

The graphs of Figure 10 and 11 displays the average classification rate of the proposed methods and existing methods. The graph of Figure 10 and 11 clearly indicates the proposed methods CE-LBP and CE-ULPB outperforms the existing methods on each database.

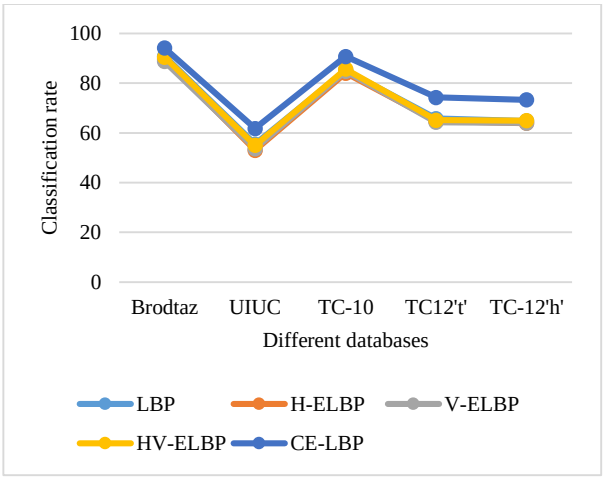

Figure 10: Average classification graph database wise on LBP based methods.

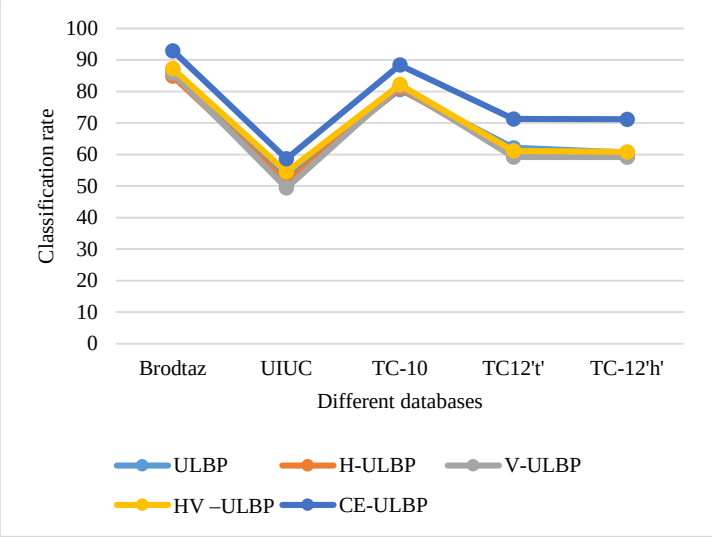

Figure 11: ULPB based average classification graph on different databases.

The following Table 4 gives the dimension of the existing and the proposed descriptors, with the type of information they capture.

Table 4: Description about the dimensions of proposed and existing descriptors.

S.No		Name of the descriptor	Dimension	Type of information	
				Isotropic	Anisotropic
1	Existing methods	$LBP_{8,1}$	256	Yes	No
2		$H\text{-}ELBP^{8,2,1}$	256	No	Yes (Partial)
3		$V\text{-}ELBP^{8,1,2}$	256	No	Yes (Partial)
4		$H\text{-}ELBP^{8,2,1}$ U $V\text{-}ELBP^{8,1,2}$	512	No	Yes(total)
5		$LBP_{(8,1)}$ U $UH\text{-}ELBP_{(8,2,1)}$ U $V\text{-}ELBP_{(8,1,2)}$	768	Yes	Yes
6	Proposed methods	$CE\text{-}LBP_{(8,1,2)}$	256	Yes (total)	Yes (total)
7		$CE\text{-}ULBP_{(8,1,2)}$	58	Yes (total)	Yes (total)

CONCLUSIONS

The present paper derived a new variant to LBP and elliptical LBP. The proposed CE-LBP captures both isotropic and anisotropic structural information without increasing any dimension. The histogram bin sizes of various methods are listed in Table 4. From Table 4, it is clearly evident that the proposed CE-LBP captures LBP, H-ELBP and V-ELBP structural information with bin size same as the above three. The present paper is also derived ULBP on the proposed CE-ULBP and performed texture classification. The results clearly state the efficacy of the proposed method over the existing methods.

REFERENCES

[1] Z. Li, G. Liu, Y. Yang, and J. You, "Scale-and rotation-invariant local binary pattern using scale-adaptive texton and subuniform-based circular shift," *IEEE Trans. Image Process.*, vol. 21, no. 4, pp. 2130–2140, Apr. 2012.

[2] K. Wang, C.-E. Bichot, C. Zhu, and B. Li, "Pixel to patch sampling structure and local neighboring intensity relationship patterns for texture classification," *IEEE Signal Process. Lett.*, vol. 20, no. 9, pp. 853–856, Sep. 2013.

[3] T. Song *et al.*, "Noise-robust texture description using local contrast patterns via global measures," *IEEE Signal Process. Lett.*, vol. 21, no. 1, pp. 93–96, Jan. 2014.

[4] T. Ojala, M. Pietik¨ainen, T. Maenp¨a¨a, Multiresolution gray-scale and rotation invariant texture classification with local binary patterns, IEEE Trans. Pattern Anal. Mach. Intell. 24 (7) (2002) 971–987.

[5] Obulesu A, JS Kiran, VV Kumar, "Facial image retrieval based on local and regional features", IEEEInternational Conference on Applied and Theoretical Computing and Communication Technology (iCATccT), pp: 841-846, 2015.

[6] V.Vijaya Kumar, A. Srinivasa Rao, YK Sundara Krishna, "Dual Transition Uniform LBP Matrix for Efficient Image Retrieval", I.J. Image, Graphics and Signal Processing, Vol.8,pp. 50-57, 2015.

[7] Ms. Shraddha D., Jumade, Prof. SheetalS.Dhande, "An Indexing and Retrieval Method Using Local Tetra Pattern for Content –Based Image Retrieval (CBIR)", International Journal of Computer Science and Information Technologies, Vol. 6,Iss.3, 2015.

[8] G. Zhao, T. Ahonen, J. Matas, and M. Pietikainen, "Rotation-invariant image and video description with local binary pattern features," *IEEE Trans. Image Process.*, vol. 21, no. 4, pp. 1465–1477, Apr. 2012.

[9] J. Ren, X. Jiang, and J. Yuan, "Dynamic texture recognition using enhanced LBP features," in *Proc. Int. Conf. Acoust., Speech, Signal Process.*, 2013, pp. 2400–2404.

[10] G. Zhao, M. Pietik¨ainen, Dynamic texture recognition using local binary patterns with an application to facial expressions, IEEE Trans. Pattern Anal. Mach. Intell. 29 (6) (2007) 915–928.

[11] K. Srinivasa Reddy, V.Vijaya Kumar, B.Eshwarareddy, "Face Recognition based on Texture Features using Local Ternary Patterns", I.J. Image, Graphics and Signal Processing,Vol.10,pp. 37-46 , 2015.ISSN: 2074-9082.

[12] J. Wu and J. Rehg, "CENTRIST: A visual descriptor for scene categorization," *IEEE Trans. Pattern Anal. Mach. Intell.*, vol. 33, no. 8, pp. 1489–1501, Aug. 2011.

[13] J. Ren, X. Jiang, and J. Yuan, "Learning binarized pixel-difference pattern for scene recognition," in *Proc. Int. Conf. Image Process.*, 2013, pp. 2494–2498.

[14] Y. Xiao, J.Wu, and J. Yuan, "mCENTRIST: A multi-channel feature generation mechanism for scene categorization," *IEEE Trans. Image Process.*, vol. 23, no. 2, pp. 823–836, Feb. 2014.

[15] J. Ren, X. Jiang, J. Yuan, and G. Wang, "Optimizing LBP structure for visual recognition using binary quadratic programming," *IEEE Signal Process. Lett.*, vol. 21, no. 11, pp. 1346–1350, Nov. 2014.

[16] J. Trefny, J. Matas, Extended set of local binary patterns for rapid object detection, in: Computer Vision Winter Workshop 2010.

[17] A. Satpathy, X. Jiang, and H. Eng, "LBP based edge-texture features for object recognition," *IEEE Trans. Image Process.*, vol. 23, no. 5, pp. 1953–1964, May 2014.

[18] J. Xu, Q. Wu, J. Zhang, and Z. Tang, "Fast and accurate human detection using a cascade of boosted MS-LBP features," *IEEE Signal Process. Lett.*, vol. 19, no. 10, pp. 676–679, Oct. 2012.

[19] Mu, Y.D., Yan, S.C., Liu, Y., Huang, T., Zhou, B.F., "Discriminative local binary patterns for human detection in personal album", Proc. IEEE Conference on Computer Vision and Pattern Recognition, pp. 1–8, 2008

[20] V. Vijaya Kumar, SakaKezia, I. SantiPrabha, "A new texture segmentation approach for medical images", International Journal of Scientific & Engineering Research (IJSER), Vol. 4, Iss.1, 2013, pp.1-5, ISSN: 2229-5518

[21] L. Nanni, S. Brahnam, A. Lumini, A local approach based on a local binary patterns variant texture descriptor for classifying pain states, Expert Syst. Appl. 37 (12) (2010) 7888–7894.

[22] J. Ren, X. Jiang, and J. Yuan, "Learning LBP structure by maximizing the conditional mutual information," *Pattern Recognit.*, vol. 48, no. 10, pp. 3180–3190, 2015.

[23] J. Ren, X. Jiang, and J.Yuan, "A chi-squared-transformed subspace of LBP histogram for visual recognition," *IEEE Trans. Image Process.*, vol. 24, no. 6, pp. 1893–1904, Jun. 2015.

[24] M. Heikkil¨a, M. Pietik¨ainen, and C. Schmid, "Description of interest regions with local binary patterns," *Pattern Recognit.*, vol. 42, no. 3, pp. 425–436, 2009.

[25] J. Ren, X. Jiang, and J. Yuan, "LBP encoding schemes jointly utilizing the information of current bit and other LBP bits," *IEEE Signal Process. Lett.*, vol. 22, no. 12, pp. 2373–2377, Dec. 2015.

[26] C. Heng, S. Yokomitsu, Y. Matsumoto, and H. Tamura, "Shrink boost for selecting multi-LBP histogram features in object detection," in *Proc. IEEE Conf. Comput. Vis. Pattern Recognit.*, 2012, pp. 3250–3257.

[27] J. Ren, X. Jiang, and J. Yuan, "Sound-event classification using pseudo-color CENTRIST feature

and classifier selection," in *Proc. Int. Workshop Pattern Recognit.*, 2016, pp. 100111C-1–100111C-5, doi: 10.1117/12.2242357.

[28] J. Ren, X. Jiang, J. Yuan, and N. Magnenat-Thalmann, "Sound-event classification using robust texture features for robot hearing," *IEEE Trans. Multimedia*, vol. PP, no. 99, p. 1, 2016, doi: 10.1109/TMM.2016.2618218.

[29] M. Pietik¨ainen, A. Hadid, G. Zhao, T. Ahonen, Computer vision using local binary patterns, Springer, London, UK, 2011.

[30] D. Huang, C. Shan, M. Ardabilian, Y. Wang, L. Chen, Local binary patterns and its application to facial image analysis: a survey, IEEE Trans. Systems, Man, And Cybernetics–part C: Applications And Reviews 41 (6) (2011) 765–781.

[31] A. Fern´andez, M. ´Alvarez, F. Bianconi, Texture description through histograms of equivalent patterns, Journal of Mathematical Imaging and Vision 45 (1) (2013) 76–102.

[32] L. Nanni, A. Lumini, S. Brahnam, Survey on LBP based texture descriptors for image classification, Expert Syst. Appl. 39 (3) (2012) 3634–3641.

[33] Li Liu, Paul Fieguth, Yulan Guo, Xiaogang Wang and Matti Pietikäinen, Local Binary Features for Texture Classification: Taxonomy and Experimental Study, *Pattern Recognition*, http://dx.doi.org/10.1016/j.patcog.2016.08.032

[34] W. Zhang, S. Shan, W. Gao, X. Chen, H. Zhang, Local gabor binary pattern histogram sequence (lgbphs): a novel non-statistical model for face representation and recognition, in: IEEE International Conference on Computer Vision (ICCV), 2005, pp. 786–791.

[35] Z. Guo, L. Zhang, D. Zhang, A completed modeling of local binary pattern operator for texture classification, IEEE Trans. Image Process. 9 (16) (2010) 1657–1663.

[36] F. Ahmed, E. Hossain, A. Bari, A. Shihavuddin, Compound local binary pattern (clbp) for robust facial expression recognition, in: IEEE International Symposium on Computational Intelligence and Informatics, 2011, pp. 391–395.

[37] T. Ahonen, J. Matas, C. He, M. Pietik¨ainen, Rotation invariant image description with local binary pattern histogram fourier features, in: Proc. Scand. Conf. Image Anal., IEEE, 2009, pp. 61–70.

[38] V. Ojansivu, J. Heikkil¨a, Blur insensitive texture classification using local phase quantization, in: A. Elmoataz, O. Lezoray, F. Nouboud, D. Mammass (Eds.), Image and Signal Processing, Vol. 5099 of Lecture Notes in Computer Science, 2008, pp. 236–243.

[39] J. Chen, S. Shan, C. He, G. Zhao, M. Pietikainen, X. Chen, W. Gao, Wld: a robust local image descriptor, IEEE Trans. Pattern Anal. Mach. Intell. 32 (9) (2010) 1705–1720.

[40] B. Zhang, S. Shan, X. Chen, W. Gao, Histogram of gabor phase patterns (hgpp): A novel object representation approach for face recognition, IEEE Trans. Image Process. 16 (1) (2007) 57–68.

[41] G. Sharma, S. ul Hussain, F. Jurie, Local higher-order statistics (lhs) for texture categorization and facial analysis, in: European Conference on Computer Vision (ECCV), 2012, pp. 1–12.

[42] R. Maani, S. Kalra, Y. Yang, Noise robust rotation invariant features for texture classification, Pattern Recognition 46 (8) (2013) 2103–2116.

[43] R. Maani, S. Kalra, Y. Yang, Rotation invariant local frequency descriptors for texture classification, IEEE Trans. Image Processing 22 (6) (2013) 2409–2419.

[44] A. Petpon, S. Srisuk, Face recognition with local line binary pattern, in: International Conference on Image and Graphics, 2009, pp. 533–539.

[45] S. ul Hussian and B. Triggs, "Visual recognition using local quantized patterns," in *Proc. Eur. Conf. Comput. Vis.*, 2012, pp. 716–729.

[46] S. Liao, A. C. S. Chung, Face recognition by using elongated local binary patterns with average maximum distance gradient magnitude, in: Proceedings of Asian Conference on Computer Vision (ACCV), 2007, pp. 672–679.

[47] L. Nanni, A. Lumini, S. Brahnam, Local binary patterns variants as texture descriptors for medical image analysis, Artif. Intell. Med. 49 (2) (2010) 117–125.

[48] P. Brodatz, Texture, 1968, "A Photographic Album for Artists and Designers" , Reinhold, New York, 1968.

[49] http://www.outex.oulu.fi/index.php?page=image_database.

[50] Svetlana Lazebnik, CordeliaSchmid, and Jean Ponce. "A Sparse Texture Representation Using Local Affine Regions", IEEE Transactions on Pattern Analysis and Machine Intelligence, Vol. 27, Iss.8, pp. 1265-1278, August 2005.